TRANSACTIONS OF THE INSTITUTE OF FLUID-FLOW MACHINERY

No. 140, 2018, 39–81

Noureddine Toujani,[a*] Nahla Bouaziz[b], Mouldi Chrigui[a], Lakdar Kairouani[a]

Performance analysis of a new combined organic Rankine cycle and vapor compression cycle for power and refrigeration cogeneration

[a] *Université Tunis El Manar, Unité de Recherche Energétique et Environnement, Ecole Nationale d'ingénieurs de Tunis, BP 37, Le Belvédère 1002 Tunis, Tunisia*

[b] *Technische Universität Darmstadt, Department of Mechanical Engineering (Dept.16)*

Abstract

Organic Rankine cycle (ORC) is considered the most used technology in low temperature heat recovery units for cogeneration (electricity and cold). In this study, the effect of the operating parameters, in particular the condensation and the vaporization temperatures on the performance of the cycle are analyzed. In addition, we developed a new combination of organic Rankine cycle and vapor compresion cycle systems to make cogeneration with a negative cold (-10–0°C), as well with a positive cold (0–10°C). Three configurations are examined and studied in terms of energy efficiency, namely the performance of each configuration including net power, refrigeration capacity and overall efficiency, the thermal efficiency for ORC and the coefficient of performance for VCC. The used working fluids are n-hexane for the ORC and R600 for the VCC. We also try to apply this new system to have the cogeneration with congelation temperatures.

The results show that, for cogeneration with negative cold, among the three configurations that we have developed, the cycle with recovery is preferable in which it has a better energy performance. For a hot spring of 1000 kW, this cycle can provide simultaneously, a maximum net work of 17 kW and a maximum net cooling capacity of 160 kW and an overall coefficient of the order of 0.3. For the production of positive cold, among the three configurations that we have developed, the basic cycle (without recovery) is the most suitable. With the same source

*Corresponding Author. E-mail adress: toujeninoureddine@gmail

of heat a maximum net work of 65 kW and a net cooling capacity in the order of 1000 kW with a global coefficient in the order of 1.05 is obtained. Our system is not only limited to be exploited for a temperature range between -10 °C and 10 °C, but can also be used with other fluids for lower temperatures (congelation temperatures).

Keywords: Organic Rankine cycle; Cogeneration; Vapor compression cycle; New combined

Nomenclature

COP_{VCC}	–	coefficient of performance for the vapor compression cycle
COP_s	–	coefficient of performance for the overall system
E	–	energy rate
H	–	enthalpy, kJ/kg
MW	–	molar mass, kg/mol
m_1	–	mass flow rate for ORC, kg/s
m_2	–	mass flow rate for VCC cycle, kg/s
P_{crit}	–	critical pressure, MPa
P_{sat}	–	saturated pressure, MPa
R_m	–	mass flow ratio
R_{pp}	–	pressure ratio for pump
R_{pc}	–	pressure ratio for compressor
s	–	entropy, kJ/kgK
T	–	temperature, °C
T_{ev}	–	vaporization temperature for VCC cycle, °C
T_{cit}	–	critical temperature
T_h	–	heating temperature for organic Rankine cycle
T_{cond}	–	condensation temperature for organic Rankine cycle
T_{sh}	–	overheating temperature for organic Rankine cycle
Q_b	–	boiler heat input (kW)
Q_{h2}	–	heat input for the exchanger 2, kW
Q_{ev1}	–	the power of the evaporator 1, kW
Q_{ev2}	–	the power of the evaporator 2, kW
Q_{ev_net}	–	the overall power evaporated by the VCC cycle, kW
W_{com}	–	working fluid pump power consumption, kW
W_{exp}	–	expander work output, kW
W_{net}	–	net work output for the overall system, kW
W_{pump}	–	working fluid pump power consumption, kW
W_T	–	mechanical work of the turbine, kW
W_C	–	mechanical work of the compressor, kW
X	–	title vapor

Greek symbols

η_{is1}	–	compressor isentropic efficiency
η_{is2}	–	expander isentropic efficiency
η_{pump}	–	working fluid pump isentropic efficiency
ΔT_{Pinch}	–	pinch temperature, °C

Subscripts

1	–	pump inlet
2	–	pump outlet
3	–	boiler output and expander inlet
4	–	expander outlet
10	–	compressor inlet
11	–	compressor outlet
11	–	condenser inlet
12	–	condenser outlet
13	–	evaporator 1 inlet
14	–	evaporator 1 outlet

Abbreviations

ARC	–	absorption refrigeration cycle
CSP	–	concentrated Solar Power
ERC	–	ejection refrigeration cycle
H1	–	exchanger 1
H2	–	exchanger 2
H3	–	exchanger 3
ORC	–	organic Rankine cycle
VCC	–	vapor compression cycle

1 Introduction

According to the International Energy Agency (IEA), solar power will be the fastest growing source of energy in the future. The growth rate of solar energy could reach more than 12% (IEA, 2010) [1]. Many countries today make decisions and political strategies in utilization of renewable resources. For that, many studies were done all over the world, Asia [2,3], Africa [4,5], America [6], whose objectives are to determine the energy potential and to choose the political strategies to improve the solar energy potential. In Europe, the Commission communication to the European Parliament and the Council for new European energy policies published in 2014 is a report entitled 'Energy Efficiency and its contribution to energy security'[7]. The target of this report is to increase the share of renewable energy up to 20% in 2020 and 30% in 2030. In fact, researches are looking for technologies that can be used to mitigate global warming around the world and reduce CO_2 emissions [8]. Energy shortage problems are facing all over the world and become more acute in all fields (metallurgy, chemical, electrical and mechanical sectors) [9,10]. So, the world faces two energy challenges: increase production to meet energy needs and reduce CO_2 emissions issued by

industrial plants. For that, the utilization of renewable energy becomes a political duty and not a strategic choice to solve energy problems. Among these renewable resources used is the solar energy, Sunil Kumar published a review as a synthetic result of studies done on energy analyses [11]. He presented various solar energy systems used in solar drying [12,13], solar air conditioning [14,15], solar refrigeration [16], solar water heating [17], and solar cooking [18]. These systems have been operated by solar photovoltaic techniques [19] and solar thermal energy used for heat and power generation [20–22].

By the integration of solar collectors at low or high temperatures, there are many robust techniques on the market such as parabolic dish collectors, parabolic trough, linear Fresnel, motor and power tower. In view of the rapid improvement in recent years, today we are talking about advanced concentrated dolar power (CSP) systems equipped with thermal energy storage (TES). In fact, CSP systems generally have been classified into two groups according to the type of concentration at the level of the absorber: a point concentration [23] and a linear concentration where rays are concentrated in an absorber in linear form like the linear Fresnel. Kuari *et al.* [24] presented these different technologies and gave the energy performances of each technology as well as the favorable conditions of use and operation. The study showed, in terms of energy performance, that solar tower has a better efficiency varying between 23 and 35% for a temperature range between 250 to 650 °C. These high temperatures offer the exploitation of this type of sensor in high power plants. In addition, it is possible to recover solar energy at low temperatures and heat discharges from the industry. The integration of these technologies serves to convert these heats into electricity and refrigeration with a lot of autonomy and economy. Frigo *et al.* [25] compared different technologies implemented in the market in terms of electrical efficiency and thermal efficiency to make cogeneration based on biomass. The comparative analysis is based essentially on three technologies: external combustion engine, internal combustion engine and ORC cycle. The study shows that the ORC system provides the best thermal and electrical efficiency. Moreover, Yufei Wang *et al.* [26] have compared the ORC and Kalina cycle to recover lost heat for power generation. The study showed that in terms of thermal efficiency, the ORC cycle is more efficient than that of the Kalina cycle. The ORC system is a thermodynamic converter that converts an external heat at a low temperature to a mechanical work at the turbine while applying an organic fluid. Several types of heat that can be used in the ORC system, including solar energy [27–29], biomass [30–31], geothermal energy [32–35] and industrial heat waste [36–38]. This technology works not only in low temperature condition but also has several advantages, e.g., low operat-

ing pressure and easy installation and maintenance. These advantages make the ORC one of the most important research topics in recent years.

Generally, the criteria for the selection of working fluids are defined by the Kyoto Protocol [39] and the Montreal Protocol [40] which based on environmental regulations. The important criteria announced by these protocols are safety, global warming potential (GWP)(<100) and no ozone depletion potential (ODP).

The working fluid for ORC is an important parameter influencing the performance of the cycle. For this reason, many researchers focus their work on most suitable fluids according to the operating parameters of the cycle (vaporization temperature and cycle type, subcritical and supercritical). Le *et al.* [41] carried out a supercritical ORC performance study for a 150 °C vaporization temperature. Eight fluids were selected to determine their performance. The fluids are: R134a, R152a, R32, R744, R1270, R290, R1234yf, and R1234ze. The result of this study showed that the maximum yield was 13.1%. For basic ORC with heat recovery, Aljundi analyzed 12 refrigerants for temperatures between 50 and 140 °C [42]. The best performance result was 13.36% for low temperatures (60–100 °C) using a preheated ORC. Tchanche *et al.* [65] analyzed this type of cycle using twenty refrigerants. They found a maximum efficiency of 14%.

The ORC system consists of a pump, evaporator, condenser and turbine. The choice of type of each component is very important in order to improve cycle efficiency. For the pumps, diaphragm pumps are most often used because of their low flow rates [43–46]. The volumes generated by these pumps are on average around 0.025 m^3/s. The efficiency of the pumps varies depending on their type. The isentropic efficiency of a diaphragm pump is 30%. On the other hand, isentropic efficiency of centrifugal pumps is higher (> 60%) [47]. As for ORC turbines, most often expanders, not turbines are used for small scale systems. According to a large number of studies based on experimental tests [48–54], the scroll expander for ORC produce powers lower than 4 kW, whereas scroll compressors deliver powers between 7 and 45 kW. For high working pressures, scroll expanders are no longer used because of their low fluid volumes [55]. Kaczmarczyk *et al.* [56] put stress on the influence of the geometry modifications of a radial microturbine on the efficiency of a micro-CHP based ORC system. The study showed that the efficiency of the integrated ORC using a microturbine increased by about three times. This produces about 17% more electrical energy. For exchangers used in ORC systems, Walraven *et al.* [57] reported that ORC systems with plate heat exchangers are more efficient than tubular heat exchangers.

To make cogeneration, several researches considered a combined system [58–61]. a study by Fadhel *et al.* [66] proposed a new method for the integration

of the adsorption cooling system with ORC to simultaneously generate cooling and electricity using a low-temperature heat source. Four different configurations were developed and compared. Several studies were devoted to combining the ORC with the adsorption cycle by different working fluids and different hot temperature sources. In [62] researchers developed a $CaCl_2/BaCl_2$ pair adsorption cycle combined with a R245fa fluid for a source temperature below 100 °C. The result showed that the energy efficiency is between 10.1 and 13.1% depending on the chosen temperature. Lu *et al.* [63] developed a new combination of ORC with adsorption for cogeneration of electricity and cold to recover heat from diesel engines at temperatures between 78 and 98 °C. The study showed the exploitation of this system according to the vaporization temperature. For a heat source released at the exhaust level of 15 kW, it is possible to recover 1 kW of electricity and 6 kW of cold. For high temperature (200–700 °C) a $SrCl_2$-$MnCl_2$/ammonia adsorption pair was selected, and this system provided 13 kW for electricity and 16 kW for refrigeration. Other researchers combined the ORC with the absorption cycle [64]. The ORC system was used to recover industrial waste heat at low temperatures. This system has been analyzed and optimized in combination with the absorption refrigeration cycle (ARC) and the ejection refrigeration cycle (ERC). The effect of the operating parameters on the thermodynamic performance of the ORC system was clarified.

Heat-activated cooling technologies such as absorption cycles have a generally low coefficient of performance (COP) for single-stage absorption cycles. ORC-VCC is very advantageous for other thermally activated cooling systems in terms of energy efficiency.

Aphornratana and Sriveerakul [67] proposed an alternative heating system which combines an organic Rankine cycle and vapor compression cycle and VCC by integrating a free-piston compressor. Both systems would use the same working fluid and share the same condenser. Wang *et al.* [68] proposed a thermally activated cooling cycle which combined ORC and VCC.

The new ORC-VCC combined system has been developed. As shown in Fig. 1, we intend to design a new architecture for poly-generation. It is an intelligent system that can be operated in four modes depending on the type of production

- **Mode 1:** Cold production. Figure 2 illustrates the basic architecture of the system. It receives a heat flow from an external renewable source in the boiler so that the ORC system can be run in order to deliver a mechanical work at the turbine. This work is transmitted totally to the VCC system compressor (turbo system compressor). The system provides us a refrigeration quantity at the evaporator as illustrated in the figure.

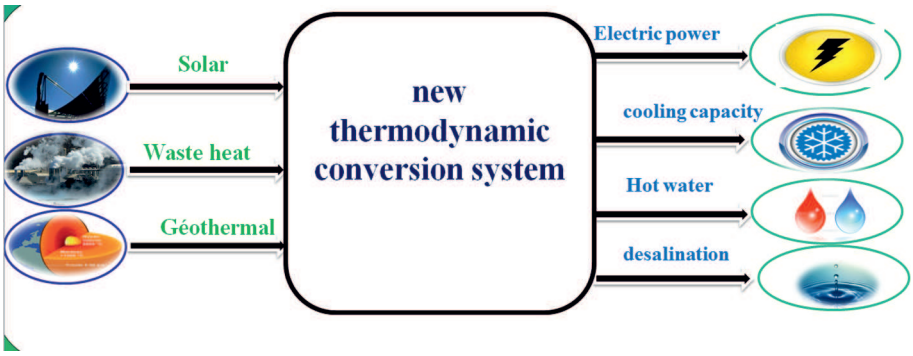

Figure 1: Purposes and objectives of the new developed system.

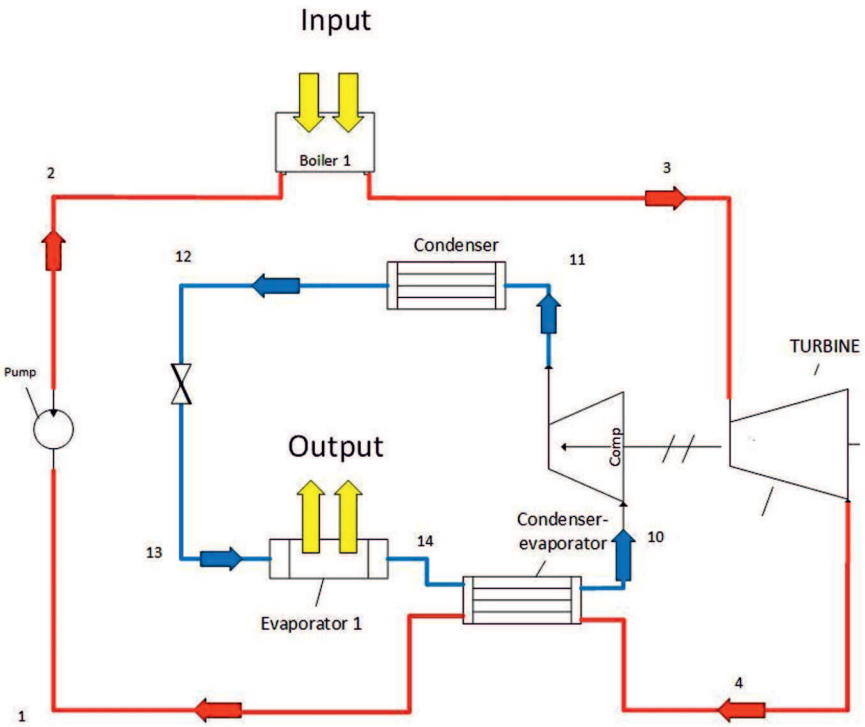

Figure 2: Cold production mode.

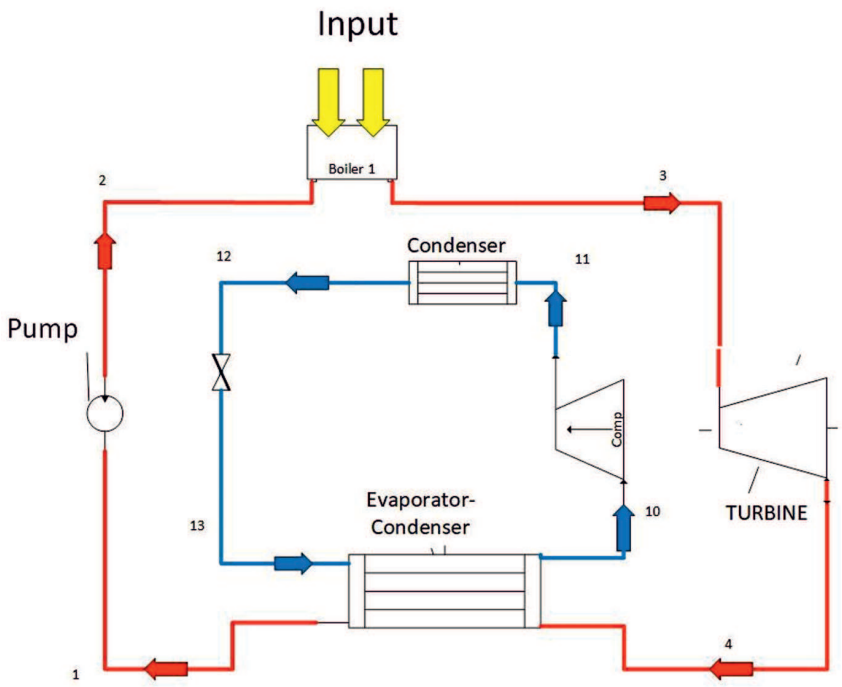

Figure 3: Electricity production mode.

- **Mode 2:** Electricity power. Figure 3 shows the basic installation. It also receives a quantity of heat from an external renewable source in the boiler to have mechanical work at the turbine, which is partially transmitted to the VCC compressor. On the other hand, the power supplied by the VCC evaporator is totally exploited by the ORC condenser. So this mode of operation requires a renewable source and provides us with electric power.

- **Mode 3:** Cogeneration (production of cold and electricity power). Figure 4 presents the basic architecture. It receives an external renewable source in the boiler. Through this source, it allows us to have mechanical work at the turbine; this is partially transmitted to the VCC compressor as mode 2. The power provided by the VCC evaporator is partially operated by the condenser ORC. So this operation mode requires a renewable source and offers an electric power by means of the ORC cycle and cooling capacity by the VCC cycle.

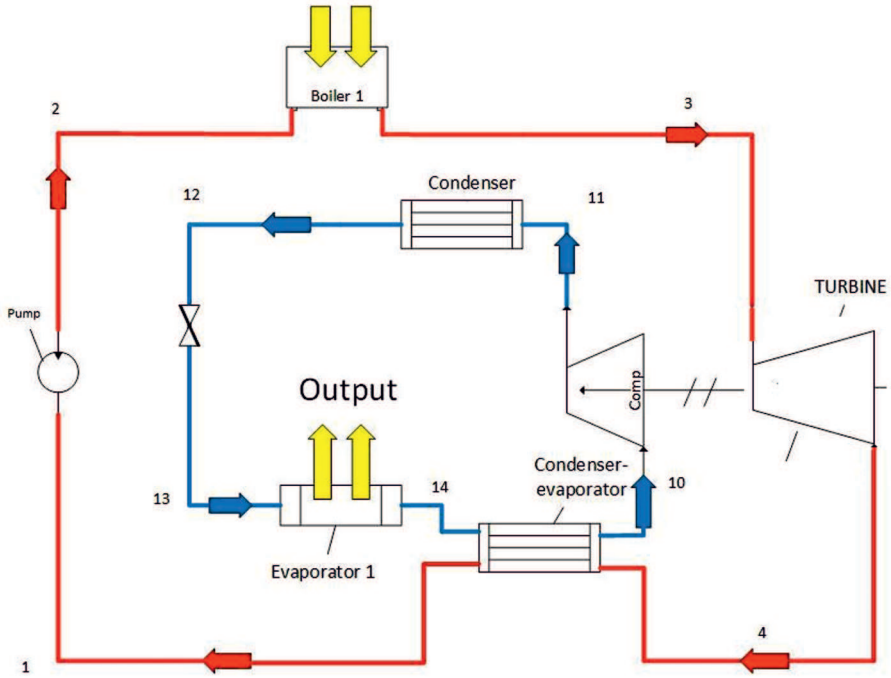

Figure 4: Cogeneration production mode.

- **Mode 4:** Tri-generation and desalination of sea water are illustrated in Fig. 5. This configuration has four circuits. An ORC circuit (that has been represented by the red color), a circuit of the VCC (in blue), a circuit in (mauve color) of the desalinated sea water and a circuit of the heated water (red color). We will couple the system with a limited renewable energy source.

In addition, each installation mode has several configurations depending on the recovery points that will be integrated later to any energy source, where we can use biomass, solar and heat rejects of industry at low temperatures (60–130 °C). The system could produce a negative and a positive cold. Thanks to its architecture, it is characterized by many combinations according to the selected fluids for the ORC and VCC cycles. It is not necessary to have the same working fluid as for the classic systems.

In this paper, we are particularly interested in studying Mode 3 which is the cogeneration of cold and electric power. The objectives of this study are:

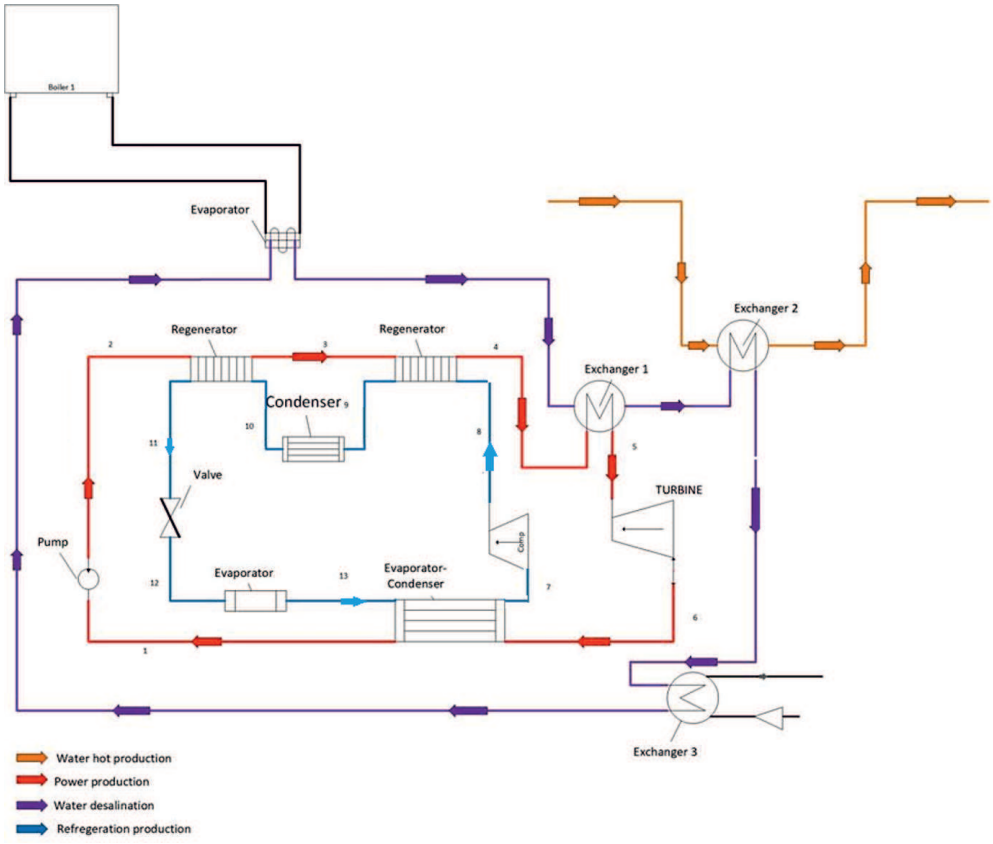

Figure 5: Tri-generation and desalination mode.

- Architectural development of the basic system.
- Development of improved configurations.
- Energy analysis and choice of fluids.
- The impact of operating parameters on energy performance.
- Analysis of the improvements for different configurations developed.
- Feasibility of cogeneration with congelation according to the type of fluid.

In this study, we will develop a new ORC combination with the VCC system in order to make cogeneration with a negative cold (-10–0°C), as well with a positive cold (0–10 °C). Three new configurations are examined and studied in terms of energy efficiency, namely the performance of each configuration including net

power, refrigeration capacity and overall efficiency, the thermal efficiency for ORC and the coefficient of performance for VCC. The working fluids are n-hexane for ORC and R600 for VCC.

2 The different techniques and means used to improve the ORC and VCC systems

Techniques and tools for improvement of an ORC system

In literature, the efficiency of the ORC system depends essentially on:

- vaporization temperature,
- condensation temperature,
- the superheated temperature,
- the working fluid.

Figure 6 illustrates and expresses the effect of these criteria on the cycle performance. In fact, the cycle in red is the basic cycle without any improvement. On the other hand, the improved cycle is marked in blue. It is clear that after these improvements, the mechanical work done in the turbine becomes more and more important. By statistical analysis, the objective will be to determine a numerical model of the ORC efficiency according to influential parameters and admitting a significant effect. Particular attention is focused on the effect of decrease of condensation temperature, which is the object of our study.

In addition, this preliminary study presents an analytical assessment of these effects in order to determine the degree of importance and these impacts on the ORC performance by a Pareto diagram.

So, we used the experiment design tool that fits well our requirements. We have chosen a complete factorial design plan for reasons of precision. As well, we will perform the study for three different fluids in order to have more confidence and precision to our results. In fact, the output results are processed by the commerecial Engineering Equation Solver (EES) software package [72]. Then with the help of Statgraphics [73] software, they are analyzed. Table 1 shows the levels of each parameter and Tab. 2 explains the experiment design including the found results of the returns.

After the statistical validation in terms of the R-squared which is in the order of 99 percent displayed in Tab. 3, it is possible to interpret our found model as the most precise. Figures 7a, 8a, and 9a confirm our result. The three models

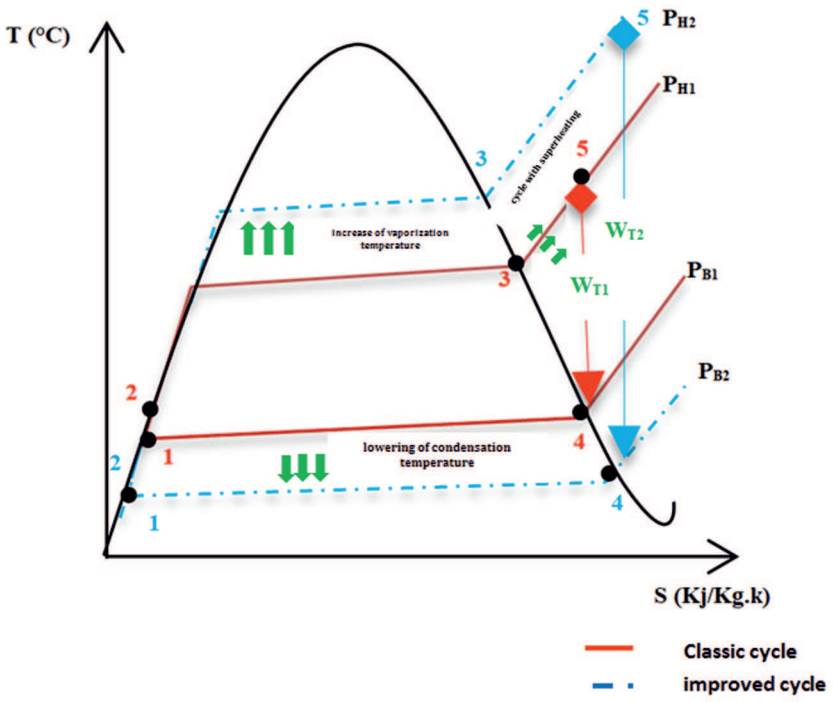

Figure 6: The impact of the parameters affecting the thermal efficiency for an ORC.

Table 1: Selected factor levels.

Factors	Low	High	Levels	Units
T_{sh}	5	25	3	°C
T_{cond}	2	18	3	°C
T_h	65	95	3	°C

found are displayed in Tab. 4. Each model presents an analytic equation of the polynomial type regrouping the parameter coefficients and the interactions between them. In addition, Figs. 7b, 8b, and 9b show the Pareto diagrams found for each fluid. It is quite clear that from the found models and Pareto diagrams for any used fluid, the most influential factors on the ORC efficiency are first the hot temperature and second the condensation temperature.

So, because our hot source is limited (by the exploitation of renewable energy)

Table 2: Experimental design matrix and result of ORC efficiency.

No.	Factor Level			Reponse ORC efficiency		
	T_{sh}	T_{cond}	T_h	Ammonia	R600	R365mfc
1	5	2	65	0.1397	0.1332	0.1318
2	15	2	65	0.1408	0.1332	0.131
3	25	2	65	0.1423	0.133	0.1301
4	5	10	65	0.123	0.1175	0.1164
5	15	10	65	0.1241	0.1173	0.1156
6	25	10	65	0.1255	0.117	0.1146
7	5	18	65	0.1061	0.1016	0.1009
8	15	18	65	0.1071	0.1013	0.09997
9	25	18	65	0.1085	0.1009	0.09903
10	5	2	80	0.1605	0.1524	0.1507
11	15	2	80	0.162	0.1525	0.1499
12	25	2	80	0.1638	0.1523	0.1489
13	5	10	80	0.145	0.1377	0.1365
14	15	10	80	0.1465	0.1377	0.1355
15	25	10	80	0.1482	0.1374	0.1345
16	5	18	80	0.1294	0.123	0.1222
17	15	18	80	0.1308	0.1229	0.1212
18	25	18	80	0.1325	0.1225	0.1201
19	5	2	95	0.1772	0.1682	0.1665
20	15	2	95	0.1794	0.1685	0.1657
21	25	2	95	0.1816	0.1685	0.1647
22	5	10	95	0.1628	0.1545	0.1532
23	15	10	95	0.1649	0.1546	0.1522
24	25	10	95	0.1671	0.1544	0.1512
25	5	18	95	0.1483	0.1407	0.1399
26	15	18	95	0.1504	0.1407	0.1389
27	25	18	95	0.1525	0.1404	0.1378

one of the main and effective techniques for improving the ORC is the lowering of condensation temperature.

Thus, 650 °C by the lowering of this temperature much more, this offers, on the one hand, a quantity of cold that can be recovered after the pumping phase. On the other hand, with this recovery, the amount of heat consumed by the boiler is minimized. So, contrary to the conventional cycle, the lowering of condensation temperature offers us a lot of mechanical work, a quantity of cold with a minimum of boiler heat. We mention also that this technique requires

Table 3: Coefficients of regression models.

Corelation/ work fluid	Ammonia		R600		R365mfc	
	P-value	regression	P-value	regression	P-value	regression
A0	–	0.0093767	–	0.0147446	–	0.0169172
A:T_{sh}	0.0000	-0.000106667	0.0000	-0.0000188194	0.0000	-0.0000638125
B:T_{cond}	0.0000	-0.00273958	0.0000	-0.00251406	0.0000	-0.00249422
C:T_h	0.0000	0.00264289	0.0000	0.00238358	0.0000	0.00230647
AA	0.0085	0.00000111111	0.0004	-0.00000122222	–	–
AB	–	–	0.0000	-0.0000015625	0.0060	-8.02083E-7
AC	0.0000	0.000003	0.0000	7.22222E-7	0.0466	-2.94444E-7
BC	0.0000	0.00000979167	0.0000	0.00000847222	0.0000	0.00000881944
CC	0.0000	-0.00000891358	0.0000	-0.0000077284	0.0000	-0.00000728395
R-s	99.9986%		99.9992%		99.999%	
R-sq	99.9981%		99.9988%		99.9986%	
S Er of Est	0.0000927435		0.000068868		0.0000718958	

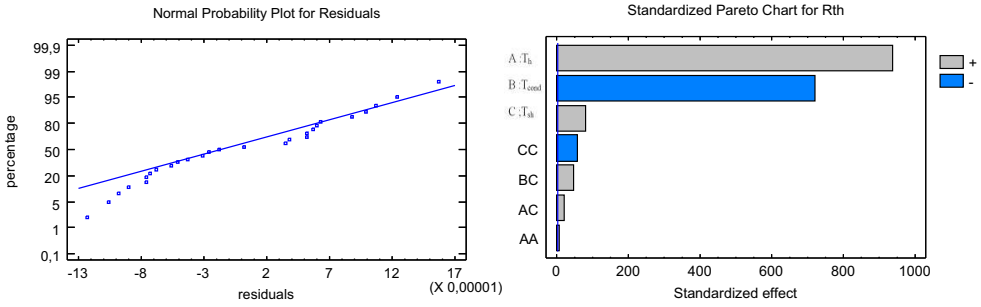

(a) (b)

Figure 7: Theoretical model plot and Pareto diagram for ammonia fluid: (a) theoretical model, (b) Pareto diagram.

a cold source to make the condensation.

Techniques and tools for improvement of a VCC system

The same approach is made for the VCC system, it is noted that the most appropriate technique to improve the cycle is to make the subcooling. Particularly this technique allows us to have more amount of produced cooling power. Also, this technique requires a cold source to cool the VCC fluid.

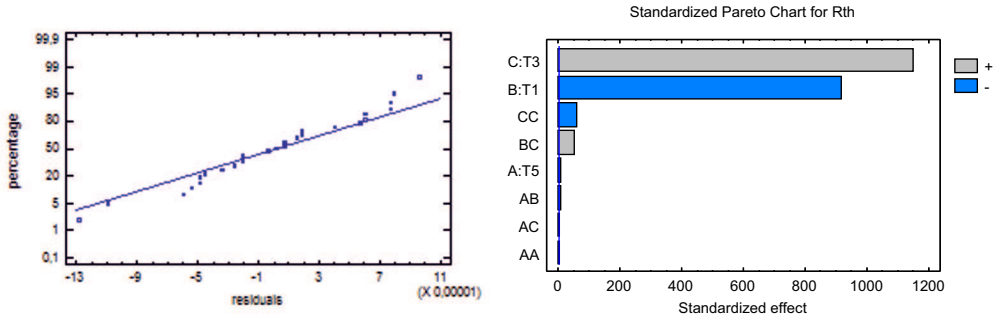

(a) (b)

Figure 8: Theoretical model plot and Pareto diagram for R600 fluid: (a) theoretical model, (b) Pareto diagram.

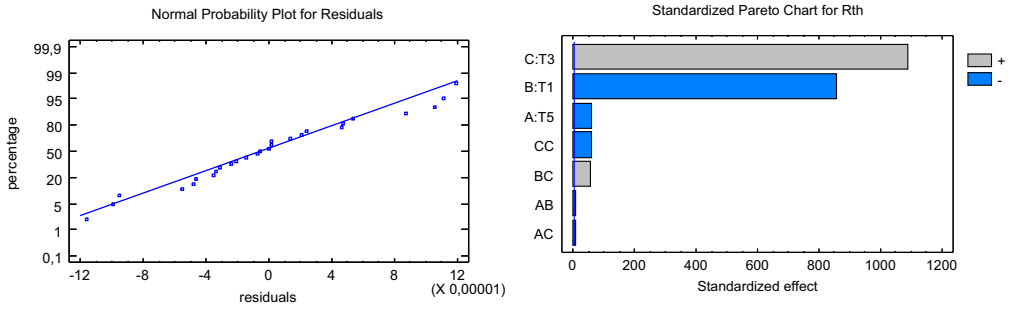

(a) (b)

Figure 9: Theoretical model plot and Pareto diagram for R365 fluid: (a) theoretical model, (b) Pareto diagram.

Recovery and enhancement diagram developed for ORC-VCC

Based on the subsequent study of ORC and VCC, we have developed recovery and enhancement diagram for ORC-VCC. This diagram tool is shown in Fig. 10. In fact, we have identified and detected the zone of recovery and improvement, so we have five zones:

- Zone 1: it is a cold recovery zone from the ORC system.
- Zone 2: it is an improvement zone based on ORC system preheating.
- Zone 3: it is a heat recovery zone from the ORC system. This recovery depends on selected fluid and operating parameters.

Table 4: Coefficients of regression models.

Selection fluid	Model
Ammonia	η_{th}= 0.0093767 – 0.000106667*T5 – 0.00273958*T1 + 0.00264289*T3 + 0.00000111111*T5^2 + 0.000003*T5*T3 + 0.00000979167*T1*T3 – 0.00000891358*T3^2
R600	η_{th}= 0.0147446 – 0.0000188194*T5 – 0.00251406*T1 + 0.00238358*T3 – 0.00000122222*T5^2 – 0.0000015625*T5*T1 + 7.22222E-7*T5*T3 + 0.00000847222*T1*T3 – 0.0000077284*T3^2
R365mfc	η_{th} = 0.0169172 – 0.0000638125*T5 – 0.00249422*T1 + 0.00230647*T3 – 8.02083E-7*T5*T1 – 2.94444E-7*T5*T3 + 0.00000881944*T1*T3 – 0.00000728395*T3^2

- Zone 4: it is an improvement zone represented by the subcooling of the fluid VCC.

- Zone 5: it is a recovery zone represented by the heat recovery of the fluid VCC.

3 System description and developed configurations

3.1 Description of the system

The objective of our study is to examine a new ORC-VCC combination to simultaneously produce electricity and cold. After developing the basic architecture [69], three different configurations are developed and analyzed. Each configuration has an ORC and a VCC systems. We will couple our facility with a limited renewable energy source, at a low temperature (100 °C). Our approach is to lower the condensation temperature between -10 and 10 °C of the ORC system so that the delivered work can be increased. So, a cold part produced by VCC will be used to condense the fluid of the ORC system. For this purpose, we will integrate an exchanger H1 which is used to condense the ORC fluid by a quantity of cold produced by VCC system.

The novelty of our system appears essentially in: the development of new ORC-VCC combination architecture, the lowering of the ORC system temperature, the possibility of cold production by the ORC system upstream of the

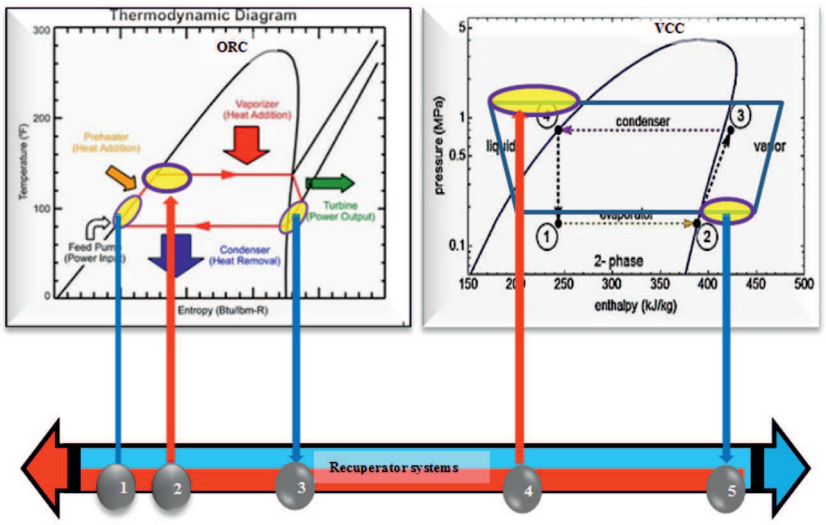

Figure 10: Developed recuperation model.

pumping phase, preheating of ORC system using VCC system fluid and new configurations based on the integration of heat recovery systems to improve overall system performance.

3.2 The different configurations developed

3.2.1 Configuration A

The cycle a is the basic configuration. We will combine the two ORC and VCC technology without any recovery for cogeneration. As shown in Fig. 11, the only combination is made at the heat exchanger H1 which serves to condense the ORC fluid. This configuration allows having cogeneration with positive or negative cold.

The operating principle is described as follows: firstly, the ORC fluid enters the boiler in order to heat it up to 100 °C by a renewable external source (biomass, industrial and solar thermal discharge, etc.). It suffices that the fluid reaches a saturated vapor phase, it enters a turbine to generate a mechanical work. This phase allows the fluid to pass from the high pressure to the low pressure. After this phase, a condensation phase is necessary to change the fluid into the liquid state. For our application, the condensation is done at low temperature which

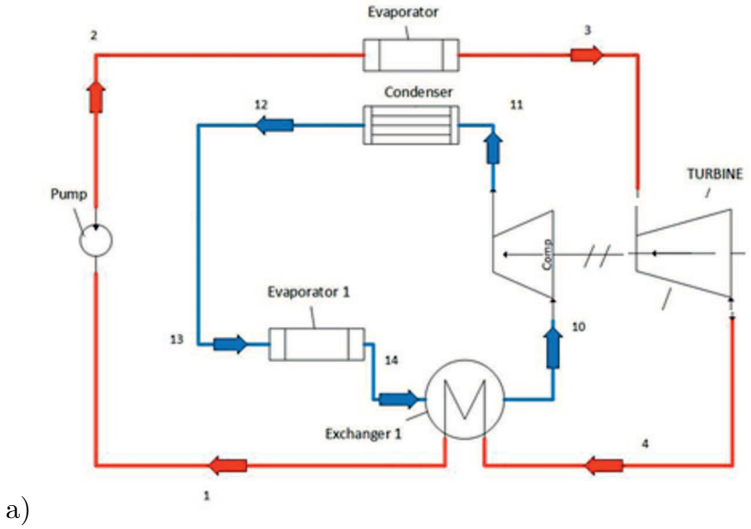

a)

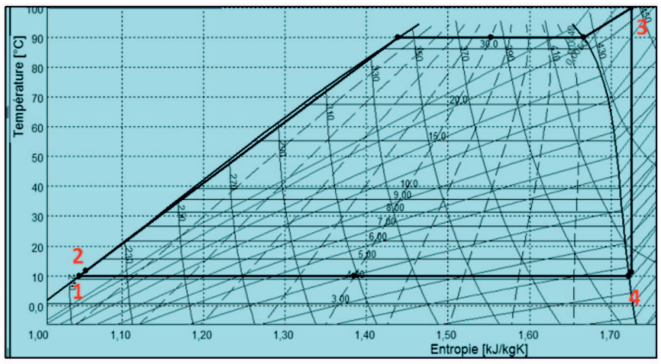

b)

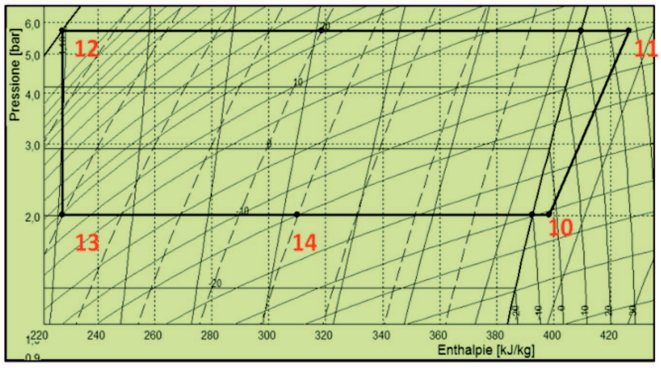

c)

Figure 11: Scheme and diagrams of the configuration A: a) scheme of the configuration A, b) T-s diagrams for ORC system, c) P-H diagrams for VCC.

requires a cold external source. For this, we have combined the ORC condenser with the VCC evaporator by integrating an H1 exchanger. For this configuration, after condensation, the fluid goes to the pumping phase which is used to pump the fluid from low pressure to high pressure. The different properties of each transformation have been detailed in Tabs. 5 and 6.

Table 5: The different phases of transformations of the ORC system.

Transfor-mations	Phases	Transformation devices	Role
1-2	pumping	pump	pumping the fluid from low pressure to high pressure
2-3	isobar heating and vaporization	boiler	heating and vaporizing the fluid
3-4	isentropic detente	turbine	detente of the fluid from high pressure to low pressure
4-1	isobar condensation	condenser	condensing fluid at constant pressure

Table 6: The different phases of transformations of the VCC system.

Transfor-mations	Phases	Transformation devices	Role
10-11	compression	compressor	compressing the fluid from low to high pressure
11-12	condensation	condenser	condensing fluid at constant pressure
12-13	detente	valve	détente of the fluid from high pressure to low pressure
13-14	first vaporization	evaporator 1	vaporizing the fluid
14-10	second vaporization	evaporator 2	vaporizing the fluid

In addition, the VCC operation is the inverse of those ORC. The VCC fluid is compressed with a mechanical compressor and then condensed at a temperature of 30 °C. In this configuration, after this phase, the fluid is released directly by an expansion valve. Then it is evaporated in two phases.

3.2.2 Configuration B

For cycle B, we kept the same basic architecture as in cycle A, except that we will integrate an H2 exchanger. This exchanger is mounted just after the pumping phase of the ORC system. Seeing that the temperature obtained at the pumping point is almost the same as the temperature of condensation which varies between -10 and 10 °C, the idea is to exploit this temperature to make the subcooling of the VCC to improve its performance. The cycle B shown in Fig. 12 is also developed to make cogeneration with a negative cold.

3.2.3 Configuration C

As shown in Fig. 13, cycle C is used also for cogeneration. Unlike the conventional ORC system, which is used only for electricity production at the turbine state, the cycle C allows the generation of electricity and cold in the ORC system. So, the configuration C is used to produce negative cold, positive cold and electricity.

We will use the heat quantity at low temperature following the pumping step in the ORC in order to produce a positive cold at 18 °C for air conditioning. For this reason, we will integrate the H3 exchanger for the heat transfer between the ambient air and the ORC fluid.

3.2.4 Description of organic Rankine cycle

The ORC systemis based on four transformations that are indicated in Tab. 5. It is composed of four components: pump, boiler, turbine and condenser. The boiler is supplied with a necessary quantity of heat. The mechanical work is provided by the turbine.

For each configuration, the ORC fluid is pumped from state 1 to state 2, then preheated and vaporized in the boiler (state 2 to 3). After flowing through the vaporization phase, the vapor (state 3) expands in a microturbine driving a generator to provide electricity. Finally, the steam from the turbine (state 4) liquefies in the exchanger H1 (state 1).

3.2.5 Description of the vapor compression cycle

This cycle also has four basic transformations, which are indicated in Tab. 6. The vaporization phase is divided into two steps; the first one is used to condense the fluid of the ORC and the second step of vaporization is to produce the cold that we will use. The VCC is constituted by a compressor, a condenser, a pressure reducer and two evaporators.

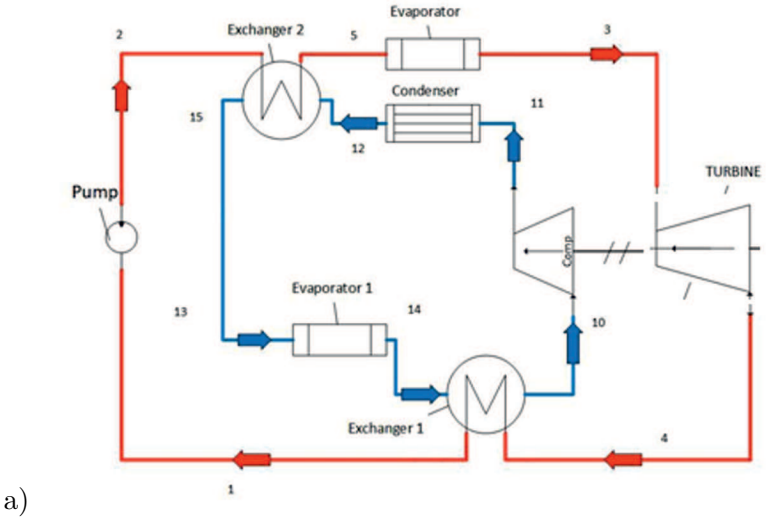

a)

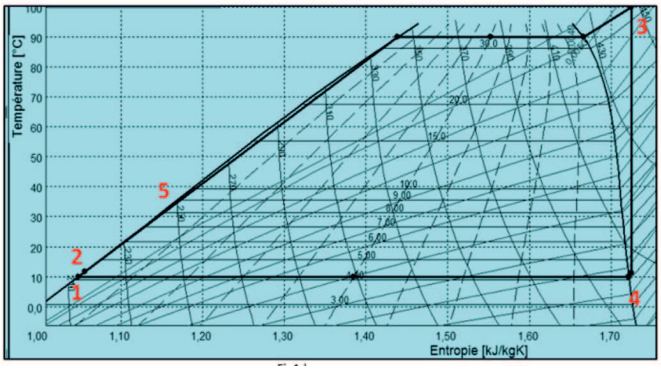

b)

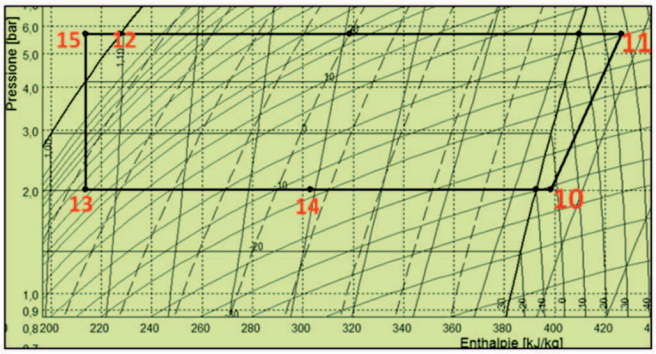

c)

Figure 12: Scheme and T-s diagrams of the configuration B: a) scheme of the configuration B, b) *T-s* diagrams for ORC system, c) *P-H* diagrams for VCC.

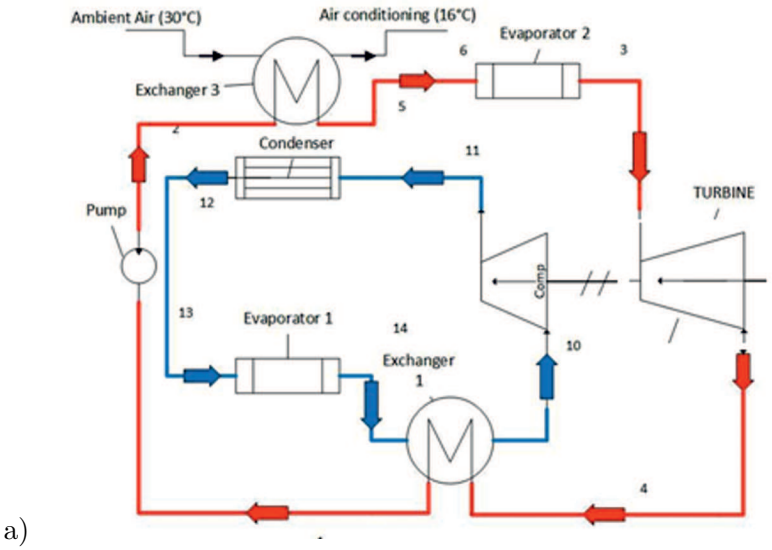

a)

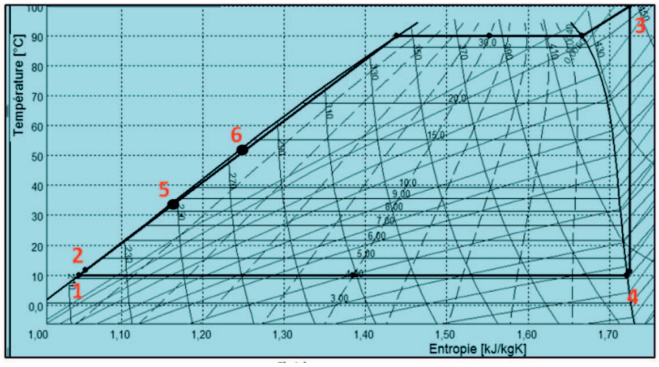

b)

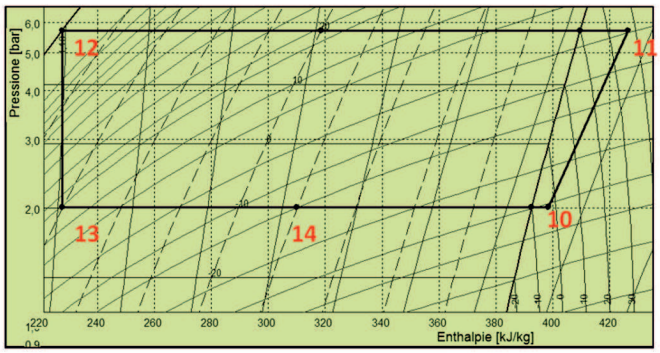

c)

Figure 13: Scheme and T-s diagrams of the configuration C system: a) scheme of the configuration C, b) *T-s* diagrams for ORC system, c) *P-H* diagrams for VCC.

For each configuration, the VCC fluid is compressed from state 10 to state 11, and then it is cooled and liquefied in a condenser (state 11 to 12). The liquid (state 12) is then released by an expansion valve. After the liquid at low pressure and low temperature, the working fluid vaporizes firstly in the evaporator (state 13 to 14) and secondly vaporization takes place in exchanger (state 14 to 10).

4 Mathematical modeling and validation

4.1 Thermodynamic modeling

During our study, we treated the thermodynamic equations as well as the resolution by a calculation program developed by the commercial Engineering Equation Solver (EES) software package [72]. As well, this software allows us to realize the different curves and tables presented in our study.

Table 7 illustrates the different thermodynamic models used throughout the work and the different configurations.

4.2 System settings and boundary conditions

The ranges of the operating parameters are shown in Tab. 8. The boundary conditions are shown in Tab. 9.

4.3 Validation of the model

The ORC and the VCC are validated respectively in Sec. 4.3.1 and 4.3.2.

4.3.1 ORC validation

The model developed for the ORC is tested with the results of Bahaa Saleh [70], which is the most appropriate configuration to validate the current model using the similar working applied fluid. The comparative results are given in Tab. 10. These results show a small deviation in thermal efficiency of the order of 2.09%. It is worth noticing that certain changes in the developed model are made for an appropriate comparison. Specifically, the condensation temperature was 40 °C and the isentropic efficiency equalled 85%.

4.3.2 VCC validation

In this section, the operation of the VCC system is enabled. The data of Nasir [71] are selected for the validation. Some changes in the model are made to have

Table 7: Thermodynamic modeling of different configurations: (1) cycle A; (2) cycle B, (3) cycle C

.

Cycle	Device	Formula
ORC	turbine	$W_T = \dot{m}_1 (h_3 - h_{4s}) \eta_{exp}$
	pump	$W_p = \dot{m}_1 \frac{(h_{2s} - h_1)}{\eta_{pump}}$
	boiler	(1) $Q_b = \dot{m}_1 (h_3 - h_2)$
		(2) $Q_b = \dot{m}_1 (h_3 - h_5)$
		(3) $Q_b = \dot{m}_1 (h_3 - h_6)$
	condenser	$Q_{cond} = \dot{m}_1 (h_4 - h_1)$
	thermal efficiency	$\mu_{orc} = \frac{(W_T - W_p)}{Q_b}$
VCC	compressor	$W_C = \dot{m}_2 \frac{(h_{11s} - h_{10})}{\eta_{comp}}$
	first evaporator	$Q_{ev1} = \dot{m}_2 (h_{14} - h_{13})$
	second evaporator	$Q_{ev2} = \dot{m}_2 (h_{10} - h_{14})$
	overall evaporator	$Q_{ev} = \dot{m}_2 (h_{10} - h_{13}) = Q_{ev1} + Q_{ev2}$
	coefficient of performance	$\mathrm{COP}_{VCC} = \frac{(Q_{ev1} + Q_{ev2})}{W_{comp}}$
overall performance of ORC/VCC	net work	$W_{net} = W_T - W_p - W_C$
	overall performance of the system	(1) and (2) $\mathrm{COP}_s = \frac{(Q_{ev1} + W_{net})}{Q_b}$
		(3) $\mathrm{COP}_s = \frac{Q_{ev1} + W_{net} + Q_{hx3}}{Q_b}$
	efficacity	(1) and (2) $E = \frac{Q_{ev1}}{W_{net}}$
		(3) $E = \frac{Q_{ev1} + Q_{hx3}}{W_{net}}$
	exchangers	exchanger 1: $Q_{hx1} = Q_{ev2} = Q_{cond}$
		exchanger 2: $Q_{hx2} = \dot{m}_1 (h_5 - h_2) = \dot{m}_2 (h_{12} - h_{15})$
		exchanger 3: $Q_{hx2} = \dot{m}_1 (h_5 - h_2) = \dot{m}_2 (h_{16} - h_{17})$

an appropriate comparison against the literature. Indeed, the temperature of the condenser is set to 30 °C. Table 11 includes the validation results along with the COP for cooling. We selected three fluids for validation, which are R245fa, R123, and R134a. Table 11 shows the discrepancy between the reference [71] and our model. The error results for R245fa, R123 and R134a are respectively 0.6%, 0.44% and 0.92%. These margins are acceptable given their low values.

Table 8: Operating parameters for all configurations.

Parameter	Value
T_3	100 °C
P_3	$P_3 = P_{sat}$ [T3]
Q_b	1 MW
T_{cond} for ORC	-10–10 °C
T_{cond} for VCC	25 °C
η_{pump}	0.65
η_{exp}	0.85
X_4	0.95–1
ΔT_{Pinch}	10 °C

Table 9: Operating parameters.

Parameter	Value
W_{net}	> 0 kW
Q_{evnet}	> 0 kW
$X4$	> 0.95
E	5-100
T_{air_in}	30 °C
T_{air_out}	18 °C
T_6	30 °C

5 Selection of the working fluid

The choice of the working fluid for an ORC or VCC system is an important criterion to improver cycle performances. Generally, there are three families of organic fluids. Figure 14 shows these three classes on a T-s diagram. The distinction between these different types essentially depends on the slope between the saturation temperature and the isentropic variation ($\Delta T/\Delta s$). If a slope is negative, the fluid is wet, such as H_2O, NH_3, and R134a. For a positive slope we speak of a dry fluid such as benzene and pentane. In the cases where the slope is infinite, it is said that this fluid is isentropic like R600 and R600a. Interesting, for the selection ORC fluid, is to have an minor heat in the evaporator in order to minimize the quantity received by the boiler. Thus, a low latent heat in the

Table 10: Validation of results for ORC system.

Fluid		Parameters				
		$T4$, °C	P_{min}, MPa	P_{max}, MPa	m_1, kg/s	η_{orc}, %
R600	Ref. [35]	48.43	0.285	1.528	17.746	12.58
	Present model	47.83	0.289	1.552	17.58	12.43
	Error	1.23	0.138	0.154	0.093	1.19
R600a	Ref. [35]	45.33	0.4038	1.998	2.423	12.12
	Present model	44.61	0.4121	1.979	2.371	11.96
	Error	1.58	0.201	0.095	2.14	1.32
R245fa	Ref. [35]	50.7	0.1801	1.267	33.424	12.52
	Present model	49.64	1.765	1.281	34.101	12.44
	Error	2.09	0.199	0.109	1.98	0.63

Table 11: Validation of results for VCC.

Fluid		COPvcc
R245 fa	Ref. [36]	6.60
	Present model	6.56
	Error	0.60
R123	Ref. [36]	6.70
	Present Model	6.67
	Error	0.44
R134a	Ref. [36]	6.45
	Present Model	6.51
	Error	0.92

condenser minimizes the amount of cold delivered by the VCC. In addition, we are looking for a fluid with a positive slope to avoid vapor having less than 0.95 of gas fraction. Thus we guarantee the elimination of erosion effects in the turbine, especially when we will lower the condensation temperature to -10 °C. Based on these criteria and conditions mentioned above, it is necessary to choose a dry or isentropic ORC fluid. We choose the n-hexane whose chemical formula is C_6H_{14}.

The thermophysical characteristics of this fluid are presented in Tab. 12.

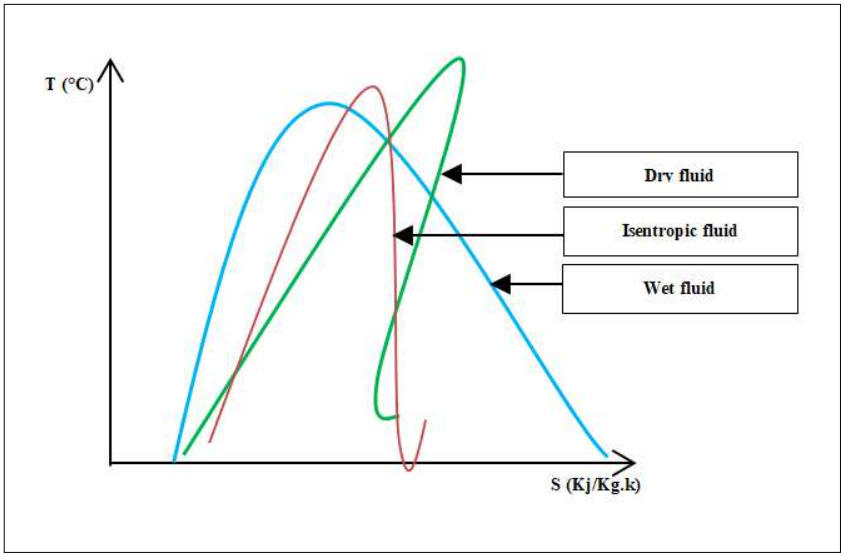

Figure 14: The different types of fluids.

Table 12: Physical and chemical properties of working fluids.

Fluid	Molecular formula	Molar mass, g/mol	Boiling temperature at 1 atm, °C	Critical temperature, °C	Critical pressure, MPa
n-hexane	C_6H_{14}	86.18	68.7	234.2	2.938
R600	CH_3 CH_3	58.00	-11.7	134.98	3.72

The R600 is selected as a working fluid for the VCC system. It is a hydrocarbon of formula C_4H_{10} crude which is found in the gas status under normal conditions of temperature and pressure. The physical characteristics of this fluid are also presented in Tab. 12. Furthermore, our choice is towards the use of n-hexane for the ORC system. This choice is essentially due to the gas fraction equal to 1 even when the condensation temperature is decreased to a low degree. This allows us to have a margin of confidence in turbine safety (avoid the erosion effects). During our study, we chose R600 as a working fluid for the VCC system. This fluid is characterized by its robustness in the market so it is used in recent

years in several researches. In addition, we find that the environmental damage is minimal.

6 Analysis and interpretation of results

6.1 Cogeneration with a negative cold

In this section, we adapt the three configurations A, B, and C to make cogeneration in electricity and negative cold between -10 and 0 °C. We are interested at analyzing the energy performance of the three cycles. The three performance indicators (η_{ORC}, COP_{vcc}, and COP_s) are studied following to the operating parameters. In addition, we will investigate the potentials delivered by each system, including net work and cooling capacity. Their evolution is going to be registered according to the ratio E and the temperature T_{ev}.

6.1.1 ORC performance energy analysis

Figure 15 shows the evolution of the ORC efficiency as a function of the temperature T_{ev} for the three configurations. The shape of the three curves demonstrates that the ORC efficiency is inversely proportional to the temperature T_{ev}. Thus, lowering of the temperature favors a better cycle efficiency. This is justified by the first thermodynamic principle. The best results for $T_{ev} = -10\,°\mathrm{C}$ found for cycle A, B, and C are 0.18, 0.185, and 0.205, respectively. As seen in this figure, the two curves of cycle A and B are parallel having a positive shift of B relatively to A. This means A that the cycle B assures a constant efficiency gain compared to A. This gain was generated by the integration of the H1 exchanger.

Table 13 shows the constant value of the amount of heat generated by this exchanger. Therefore, it can be concluded that the addition of H1 in our system has a positive effect on improving ORC system efficiency.

On the other hand, the shape of the cycle C has a different slope compared to B and A. We observe that the cycle C is the most efficient. The efficiency of this cycle, compared to other cycles, becomes the highest when T_{ev} reaches -10 °C.

The variation of the efficiency gain is due to the variation of the amount of heat recovered by the exchanger H2 as a function of T_{ev}. Table 10 shows values of Q_{h2} as a function of T_{ev}. The increase in Q_{h2} is mainly due to the decrease of H2 which favors a significant enthalpic difference (h_2-h_1) and leads to a significant value of Q_{h2}.

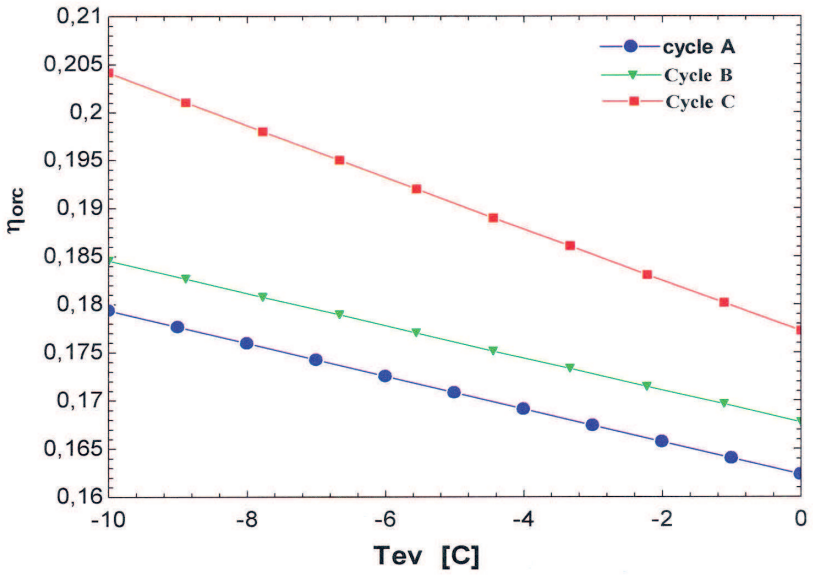

Figure 15: Variation ORC efficiency as a function of T_{ev}.

Table 13: Change of cycle parameters with E.

E –	T_{ev} °C	Q_{h2} kW	Q_{h3} kW	m_1 kg/s	m_2 kg/s	m_3 kg/s	X_{13}	W_{net} kW	R_m –	Q_{ev2} kW	Q_{ev1} kW
Cycle A											
1	0	–	–	1.904	2.730	–	0.1540	50.09	0.6970	837.6	50.090
10	0	–	–	1.904	3.343	–	0.1540	30.60	0.5690	837.6	249.20
30	0	–	–	1.904	3.662	–	0.1540	11.77	0.5200	–	353.10
Cycle B											
1	-10	20.09	–	1.865	2.700	–	0.1897	22.57	0.6909	837.1	22.57
	0	20.32	–	1.943	2.730	–	0.1346	53.39	0.7116	854.6	53.39
10	-10	21.78	–	1.868	2.927	–	0.1897	9.360	0.6383	838.5	93.60
	0	25.24	–	1.952	3.392	–	0.1346	26.95	0.5755	858.8	269.5
Cycle C											
10	-10	–	67.41	2.080	3.210	–	0.2010	13.25	0.6478	933.3	–
	0	–	22.23	2.080	3.633	1.841	0.1540	27.93	0.5725	914.8	–

6.1.2 Energy analysis of VCC performance.

Figure 16 illustrates the evolution of COP_{vcc} as a function of cold temperature T_{ev}. It is obvious that by decreasing the temperature T_{ev}, the COP_{vcc} is continuously reduced. When T_{ev} is lowered, the input enthalpy value at the compressor increases, which makes it possible to have a large compressor work W_C and leads

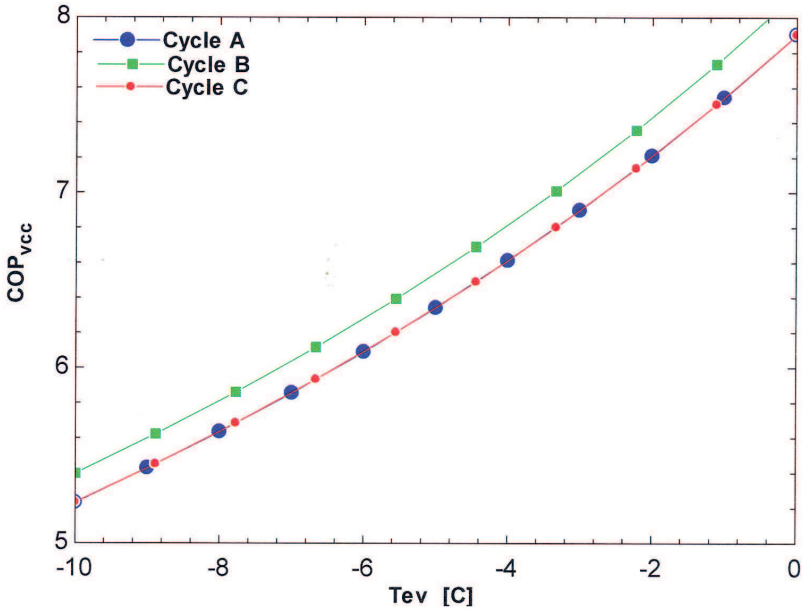

Figure 16: Variation of COP_{VCC} as a function of T_{ev}.

to a reduction in the COP_{VCC}. It is also observed that the two curves A and C are confounded. Whereas, the two configurations have the same VCC global architectures as shown in Figs. 10 and 12, the addition of the exchanger H2 for the configuration C, is only acting on the ORC yield to produce cold. It has no effect on the VCC.

The configuration B exhibits some improvement compared to the cycle A. This improvement is due to a gain in refrigeration. In fact, the addition of H2 directly influences the value of COP. This exchanger adds a subcooling phase. After the condensation phase, the VCC fluid will be cooled by a condensing temperature that is set at 25 °C down to a temperature of 18 °C, which allows us to find a lower enthalpy value at the outlet of the exchanger than that of the condenser. Therefore, more cooling capacity Q_{ev} is obtained. Therefore, the

addition of the H2 exchanger has a positive effect on Q_{ev}. It is for this reason that an improvement is made on the coefficient COP_{VCC} for cycle B.

6.1.3 Energy analysis of overall performance

The two Figs. 17 and 18 represent the effect of the vaporization temperature and the ratio E on the overall performance of the three configurations A, B, and C. Since our system provides two types of energy (electricity and cooling power) and since these are determined by the user according to his needs, we have defined a coefficient named E which is a ratio between these two types of energy. So, according to the demand of the user for electricity and cold, we fix the value of E. In addition, the COP is a performance indicator of the overall system. Its value can exceed 1, for this reason we have to define it not as efficiency but as a coefficient of performance. This indicator is determined by the law of entry/ exit of our system. In fact, the system receives a heat source to operate the boiler Q_b and thus provides us with two types of energy (electrical energy and refrigeration). Moreover, in literature, this indicator is often used by several researches to determine the overall performance of a system providing these two types of energy.

By increasing T_{ev}, the COP_s becomes continuously increasing this increase varies from one cycle to another. In fact, when T_{ev} increases the work generated by the compressor is reduced. As a result, the net work provided by the system is increased. Thereafter, the COP_s increases. This is why the effect of T_{ev} is significant for COP_s.

In addition, the two figures illustrate the effect of variation of E on COP_s. This effect is significant. When we increase E, Q_{ev} is augmented. This leads to an increase of COP_s. So we can interpret that the COP_s depends not only on the temperature T_{ev} but also on the value of E.

As can be seen in these two curves, the cycle A has low COP_s, because this cycle does not admit any recovery point. The integration of the H2 exchanger in the B cycle improves the COP_s. We observed that cycle B has COP_s better than A. Cycle B has a positive and constant gain compared to A. This gain is the value of the amount of heat recovered by A, as shown in Tab. 6.

For cycle C, the addition of the H3 exchanger also influences the COP_s. We observe that this cycle is the most efficient for $E = 10$. When the value of the ratio E tends to 100, it is found that the two curves of the cycles B and C intersect at a critical temperature of T_{ev} which is equal to 5.5 °C. It means that the increase of E reduces the efficiency of cycle C and improves the efficiency of cycle B. This interpretation is reasonable because the increase of E promotes

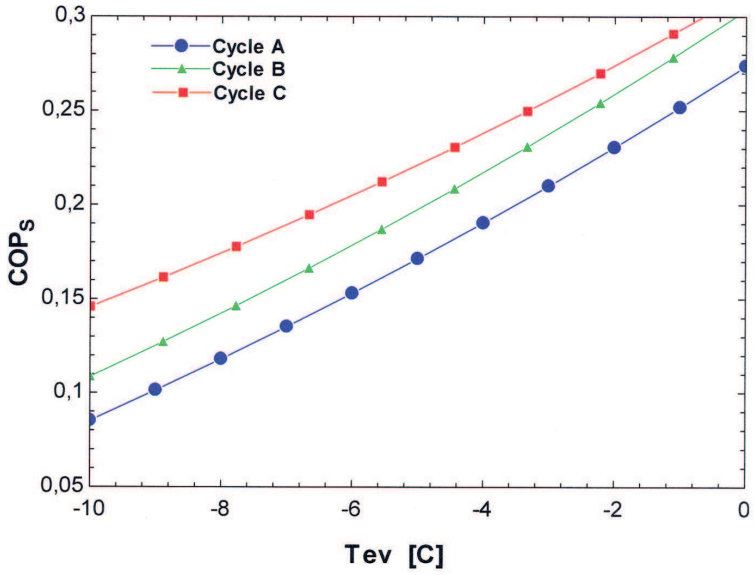

Figure 17: Variation of COPs as a function of T_{ev} for E equal to 10.

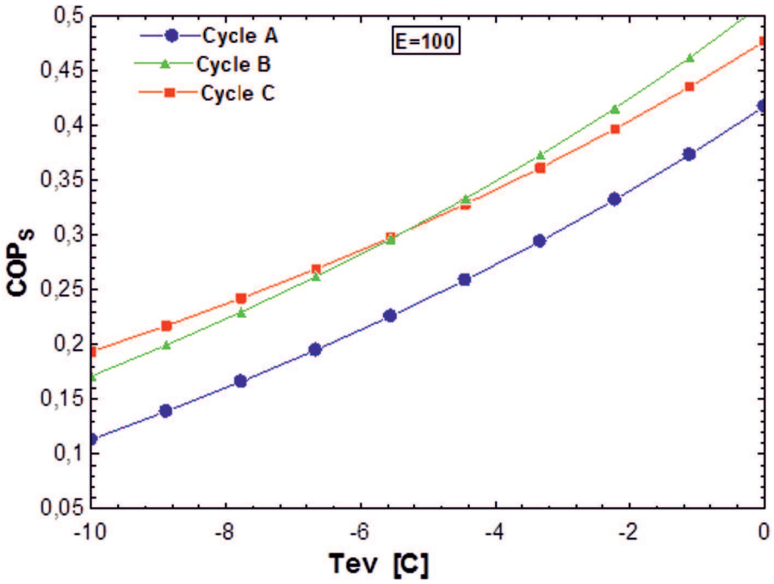

Figure 18: Variation of COPs as a function of T_{ev} for E equal to 100.

the growth of Q_{ev}. We noticed that the H2 exchanger integrated in cycle B has a positive effect on the value of Q_{ev}. On the other hand, for cycle C, an increase of Q_{ev} acts to increase the flow of VCC fluid. The latter makes it possible to increase the work consumed by the compressor. In addition, when increasing T_{ev}, the amount of heat (recovered by the exchanger H3) is decreased. So, the coefficient COP_s, decreases as well.

6.1.4 Analysis energy productivity in cold and electricity

From the point of view of the energy potential of cold and electricity produced by the various configurations, we will analyze the evolution of net refrigeration quantity Q_{ev} produced as a function of the ratio E for T_{ev} equal to -10 ° C. It can be observed from Fig. 19 that the shape of three curves has an increasing exponential form. The effect of E is significant for Q_{ev}. It is less than 50 for which the evolution of Q_{ev} is very fast. For example, for cycle C and with E between 5 and 50, an increase of 100 kW of Q_{ev} is noted. Beyond this interval, the variation of Q_{ev} becomes very slow and almost constant. The effect of E is then considered negligible. The three cycles A, B, and C have three zones of evolutions zone 1 is: the zone of rapid evolution of Q_{ev}, zone 2 is the transition zone of Q_{ev}, and zone 3 materializes a slow evolution of Q_{ev}. The cycles A, B, and C have a common transient area between 25 and 50. Therefore, the optimum amount of cold gain produced in this area is illustrated in the Fig. 19. The maximum value of COP_s is given by the numerical application of the equation shown in Tab. 7. Since the amount of heat Q_b is assumed as 1000 kW for T_{ev} equal to -10°C, maximum values of Q_{ev} are set for each configuration.

In a similar way, the evolution of the net work, W_{net}, as a function of the ratio E is illustrated in Fig. 20. It is observed that the shape of the three curves has the form of decreasing exponential. Therefore, maximum net work values recorded in cycles A, B, and C are respectively 11.6, 16.8 and 19.8 kW.

6.2 Cogeneration production with positive cold

In this part, we will analyze the performance of the system to make cogeneration with positive cold between 0 and 10 °C. The cycle a is the only system that can provide positive cold. In fact, when the temperature is raised to 10 °C, the cycles B and C have pinch problems at the exchangers H2 and H3 where the difference in the proposed pinching temperatures cannot be respected ($\Delta T_{Pinch} = 10$ ° C). For that, we will select the cycle A.

Figure 21 shows the variation of COP_s versus T_{ev} with different values of E.

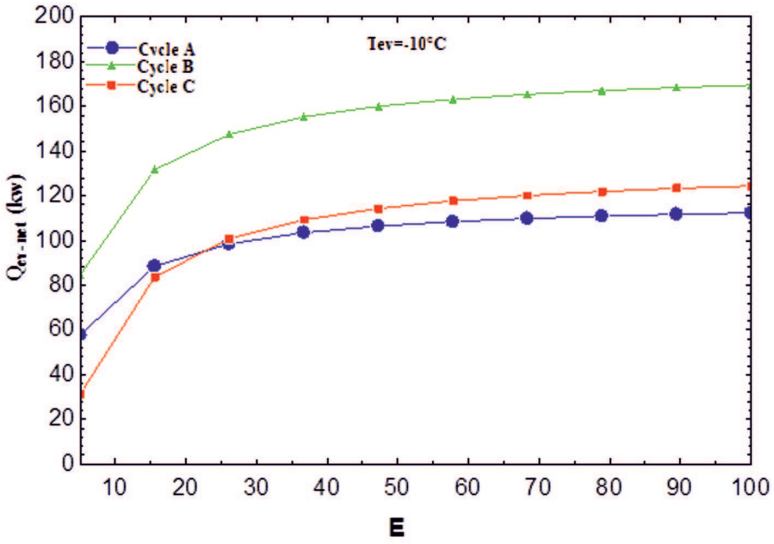

Figure 19: Variation of quantity Q_{ev} net production as a function of E for T_{ev} equal to -10 °C.

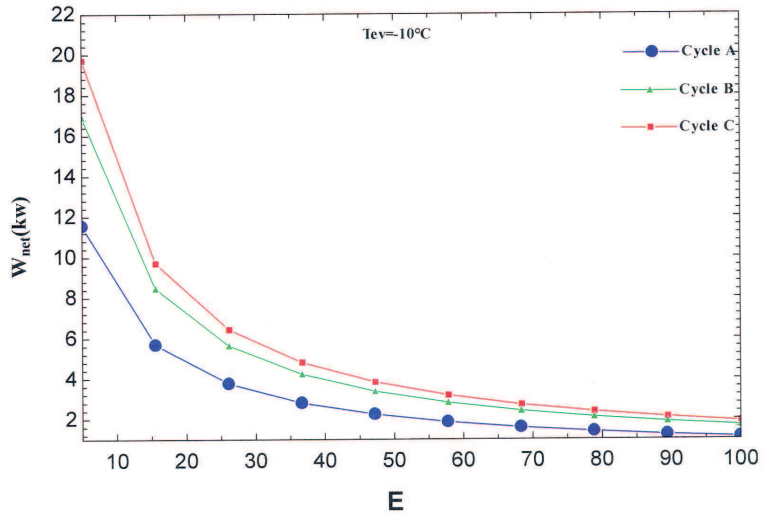

Figure 20: Variation of W_{net} as a function of E for T_{ev} equal to -10 °C.

It can be seen that the values of the COP_s are higher than values reached for the negative cold. The increase of T_{ev} leads to better performances. For example, for $T_{ev} = 10\,^{\circ}\mathrm{C}$ and $E = 100$, the value of COP_s is 1.075 and 0.5 for $E = 10$.

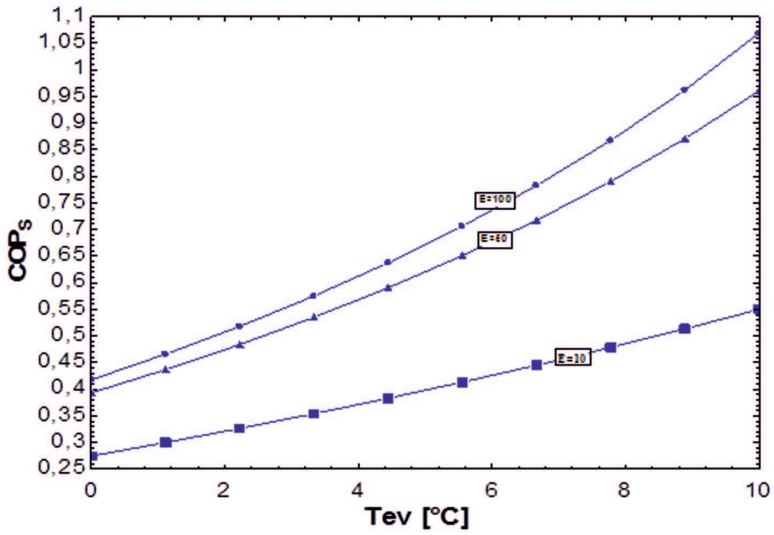

Figure 21: Variation of COPs as a function of T_{ev} for cogeneration with positive cold.

It is noted that the variation of the two curves which represent the efficiencies for $E = 50$ and $E = 100$ is negligible. On the other hand, the curve which represents the efficiency $E = 10$ shows a significant variation.

For E between 10 and 50, the efficiency has a significant effect on the COP_s. Beyond these limits, the efficiency range becomes negligible. For energy productivity, in terms of net work and net refrigeration, the amount for configuration a is shown in Figs. 22 and 23. Figure 22 shows the variation of W_{net} as a function of E and T_{ev}. It is observed that the maximum amounts that can be produced for T_{ev} of 2 °C, 5°C and 10 °C are respectively 40.48 and 63 kW. Figure 23 shows the variation of Q_{evnet} as a function of E and T_{ev}. The maximum amounts that can be produced for T_{ev} of 2 °C, 5 °C, and 10 °C are respectively 500, 660, and 1060 kW.

6.3 Other applications with lower temperature (congelation)

Our system is not only limited to be exploited for a temperature range between -10 and 100 °C but can be also used for lower temperatures reaching congelation temperatures. It all depends on the choice of the working fluid for ORC and VCC which affects the amount of cold produced.

We have selected three combinations of ORC-VCC working fluid that respond well to producing lower refrigeration temperatures. The three combinations are

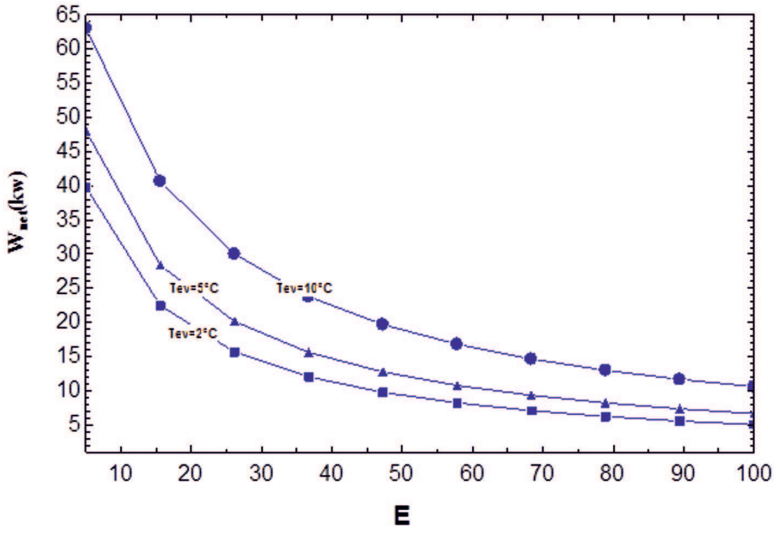

Figure 22: Variation of W_{net} as a function of E for cogeneration with positive cold.

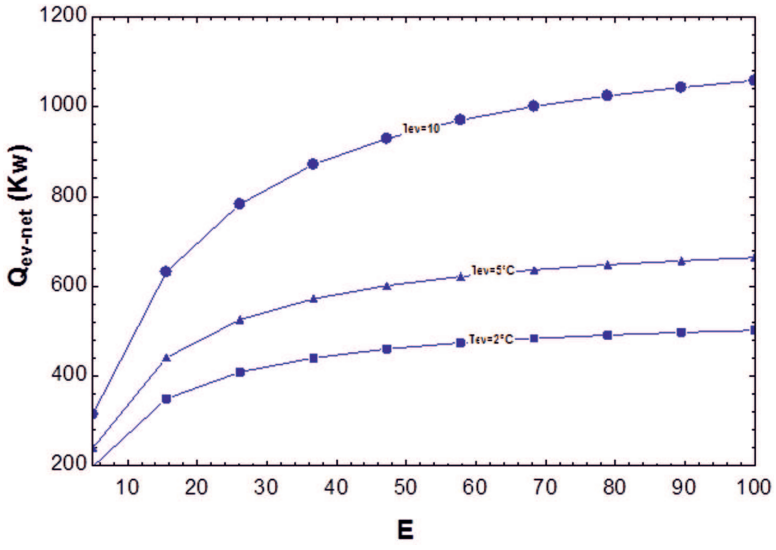

Figure 23: Variation of net Q_{ev} as a function of E and T_{ev} for cogeneration with positive cold.

ammonia-R600, R245fa-134a and R245fa-ammonia. We feed our installation with a hot spring of 100 °C. The configuration chosen for this test is configuration B. The grids shaded show the limit temperatures for each fluid used. Beyond this

threshold temperature, the net produced work becomes negative otherwise it is necessary to a backup electrical source when it is operating at the threshold temperature. Table 14 shows some other combinations of the fluids that give us lower temperature.

Table 14: Results of cogeneration with congelation in ORC-VCC systems operating on different fluids.

ORC- VCC fluids	Qev_{net}, kW	Rm	COP_s	T_1, °C	W_{net}, kW	Q_b, kW
Ammonia-R600	100	2.3710	0.4025	-17	1.746	416.1
		2.4280	0.3939	-10	14.09	414.9
		2.5240	0.3673	0	29.62	414.6
	200	2.0150	0.5887	-7.931	1.3930	414.7
		2.0670	0.5785	0	17.15	414.6
		2.1280	0.5554	10	31.9	415.5
R245fa-134a	100	0.4986	0.5622	-10	2.183	239.3
		0.5281	0.5559	0	13.4	238.7
		0.5462	0.5455	5.862	18.85	238.7
	200	0.3976	0.9199	-0.3448	0.2924	238.7
		0.4080	0.9228	4.828	7.565	238.7
		0.4101	0.9229	5.862	8.923	238.7
R245fa-ammonia	100	3.6010	0.5264	-13.45	0.1965	–
		3.6870	0.5239	-5.172	9.591	–
		3.7450	0.5172	0.3448	14.86	–

It is observed that for the combination ammonia-R600 with a cooling quantity of 100 kW, the system offers us a threshold temperature in the order of -17 °C with a hot power of 416.1 kW. It is also noted that this hot power Q_b varies slightly as a function of the refrigerating temperature. This is reasonable considering the integration of the H2 exchanger used to preheat the ORC fluid; it is the advantage of our installation compared to other conventional cycles. It is also noted that during passage of a cooling capacity 100 to 200 kW, the threshold temperature is reduced and becomes -7 °C. This is obvious, since the increase in Q_{ev} leads to an increase in flow circulated in the VCC system, which leads to an increase in W_C and subsequently a decrease in W_{net}.

7 Conclusions

The energy performance of power and refrigeration cogeneration through an organic Rankine cycle (ORC) with a vapor compression cycle (VCC) by a new

combination system is examined. We can use a low temperature energy source. Two cases of refrigeration and cogeneration are analyzed, including cases of cogeneration (-10, 10 °C) and congelation (0, -17 °C) are studied.

The effects of the system parameters, including the condensation and vaporization temperatures for ORC and VCC and the ratio E on cycle performance parameters such as thermal efficiency, specific refrigeration, net work output, and global system performance, are investigated.

According to the analysis and the investigation carried out during this study, the main interpretations retained are:

- The results show that operating parameters have a significant effect on performance. This effect differs from one case to another (positive or negative refrigeration) and according to the installed configuration (cycle A, B, and C).

- The three developed configurations based on the integration of recovery exchangers noted improvements in overall performance. These improvements also differ from one cycle to another, which makes it possible to say that the place of integration of the exchangers has an effect on the performances.

- The results show that for cogeneration with negative cold, among the three configurations that have been developed, the cycle B has the best energy performance. For a hot spring of 1000 kW, the cycle B can provide simultaneously a maximum net work output of 17 kW and a maximum net cooling capacity of 160 kW and an overall coefficient of the order of 0.3.

- For the production of positive cold, among the three configurations that have been developed, the cycle a is the most suitable, where we can obtain with the same source of heat a maximum net work output of 65 kW and a net cooling capacity of the order of 1000 kW with a global coefficient of the order of 1.05.

- Our system is not only limited for a temperature range between -10 °C and 10 °C but can be used for lower temperatures, reaching congelation temperatures. Ammonia and R600 are the most suitable two fluids for this state (congelation), which allows us to provide a temperature of -17 °C.

Received in March 2018

References

[1] International Energy Agency (IEA), 2010. International Energy Outlook-Highlights. IEA, Washington D.C.

[2] . Mohanty S: *Forecasting of solar energy with application for a growing economy like India: Survey and implication.* Renew. Sust. Energ. Rev. **78**(2017), 539–553.

[3] Nematollahi O.: *A feasibility study of solar energy in South Korea.* Renew. Sust. Energ. Rev. **77**(2017), 566–579.

[4] Ozoegwu C.G.: *The status of solar energy integration and policy in Nigeria.* Renew. Sust. Energ. Rev. **70**(2017), 457–471.

[5] Aliyuae A.S., Dada J.O., Adam I.K.: *Current status and future prospects of renewable energy in Nigeria.* Renew. Sust. Energ. Rev. **48**(2015), 336–346.

[6] Herche W.: *Solar energy strategies in the U.S. utility market.* Renew. Sust. Energ. Rev. **77**(2017), 590–595.

[7] Communication from the Commission to the European Parliament and the Council: Energy Efficiency 610 and its contribution to energy security and the 2030 Framework for climate and energy policy. Brussels, 611 23.7.2014 COM(2014) 520 final.

[8] Sarbu I., Sebarchievici C.: *General review of solar-powered closed sorption refrigeration systems.* Energ. Convers. Manage. **105**(2015), 403–422.

[9] Gingerich D.B., Mauter M.S.: *Quantity, quality, and availability of waste heat from United States thermal power generation.* Environ. Sci. Technol. **49**(2015), 14, 8297–8306.

[10] Chen CL, Li PY, Le SNT: *Organic Rankine cycle for waste heat recovery in a refinery.* Ind. Eng. Chem. Res. **55**(2016), 12, 3262–3275.

[11] Sansaniwal S.K., Sharma V.: *Energy and exergy analyses of various typical solar energy applications: a comprehensive review.* Renew. Sust. Energ. Rev. **82**(2018), 2, 1576–1601.

[12] Bolaji B.: *Exergetic analysis of solar drying systems.* Natural Resources **2**(2011), 92–97.

[13] Fudholi A., Sopian K.B., Othman M.Y., Ruslan M.H.: *Energy and exergy analyses of solar drying system of red seaweed.* Energy Buildings **68**(2014), Pt. A, 121–129.

[14] Gunhan T., Ekren O., Demir V., Sahin A.S.: *Experimental exergetic performance evaluation of a novel solar assisted LiCl–H2O absorption cooling system.* Energy Buildings **68**(2014), Pt. A, 138–146.

[15] Siddiqui F.R, El-Shaarawi M.A.I., Said S.A.M.: *Exergo-economic analysis of a solar driven hybrid storage absorption refrigeration cycle.* Energ. Convers. Manage **80**(2014), 165–172.

[16] Bouaziz N., Lounissi D.: *Energy and exergy investigation of a novel double effect hybrid absorption refrigeration system for solar cooling.* Int. J. Hydrogen Energ. **40**(2015), 13849–13856.

[17] Gang P., Guiqiang L., Xi Z, Jie J., Yuehong S.: *Experimental study and exergetic analysis of a CPC-type solar water heater system using higher-temperature circulation in winter.* Sol. Energy **86**(2012), 1280–1286.

[18] Shukla S.K., Gupta S.K.: *Performance evaluation of concentrating solar cooker under Indian climatic conditions.* In: Proc. 2nd Int. Conf. on Energy Sustainability, Jacksonville, 10–14 Aug. 2008.

[19] Naik P.S, Palatel A.: *Energy and exergy analysis of a plane reflector integrated photovoltaic-thermal water heating system.* ISRN Renew. Energy 2014:1–9. http://dx.doi.org/10.1155/2014/180618

[20] Wu J., Zhu D., Hua W., Zhu Y.: *Exergetic analysis of a solar thermal power plant.* Adv. Mater. Res. **724-725**(2013), 156–162.

[21] Ehtiwesh I.A.S., Coelho M.C., Sousa A.C.M.: *Exergetic and environmental life cycle assessment analysis of concentrated solar power plants.* Renew. Sust. Energ. Rev. **56**(2016), 145–155.

[22] Cau G., Cocco D.: *Comparison of medium size concentrating solar power plants based on parabolic through and linear Fresnel collectors.* Energy Procedia **45**(2014), 101–110.

[23] Reddy V.S., Kaushik S.C., Tyagi S.K.: *Exergetic analysis and performance evaluation of parabolic dish Stirling engine solar power plant.* Int. J. Energy Res., 2012, doi.org/10.1002/er.2926

[24] Kuavi S., Trahan J., Goswami D.Y., Rahman M.M., Stefanakos E.K.: *Thermal energy storage technologies and systems for concentrating solar power plants.* Prog. Energ. Combust. **39**(2013), 4, 285–319.

[25] Frigo S., Gabbrielli R., Puccini M., Seggiani M., Vitolo S.: *Small-Scale Wood-Fuelled CHP Plants: a Comparative Evaluation of the Available Technologies.* Chem. Eng. Transact. **37**(2014), DOI: 10.3303/CET1437142

[26] Wang Y., Tang Q., Wang M., Feng X.: *Thermodynamic performance comparison between ORC and Kalina cycles for multi-stream waste heat recovery.* Energ. Convers. Manage. **135**(2017), 63–73.

[27] Roy J.P., Mishra M.K., Misra A.: *Performance analysis of an Organic Rankine Cycle with superheating under different heat source temperature conditions.* Appl. Energ. **88**(2011), 9, 2995–3004.

[28] Cong C.E., Velautham S., Darus A.S.: *Solar thermal organic Rankine cycle as a renewable energy option.* Jurnal Mekanikal (Journal Mechanical, University Technology Malaysia) **20**(2005), 68–77.

[29] Techanche B.F., Papadakisa G., Lambrinosa G., Frangoudakisa A.: *Fluid selection for a low-temperature solar organic Rankine cycle.* Appl. Therm. Eng. **29**(2009), 2468–2476.

[30] Drischer U., Bruggemann D.: *Fluid selection for the organic Rankine cycle (ORC) in biomass power and heat plants.* Appl. Therm. Eng. **27**(2007), 223–228.

[31] Daniel Walraven, Ben Laenen, William D'haeseleer: *Minimizing the levelized cost of electricity production from low-temperature geothermal heat sources wit ORCs: Water or air cooled.* Appl. Energ. **142**(2015), 144–153.

[32] Heberle F, Brüggemann D.: *Exergy based fluid selection for a geothermal organic Rankine cycle for combined heat and power generation.* Appl. Therm. Eng. **30**(2010), 11-12, 1326–1332.

[33] Yang Y., Huo Y., Xia W., Wang X.: *Construction and preliminary test of a geothermal ORC system using geothermal resource from abandoned oil wells in the Huabei oilfield of China.* Energy **140**(2017), 1, 633–645.

[34] Bina S.M., Jalilinasrabady S., Fujii H.: *Thermo-economic evaluation of various bottoming ORCs for geothermal power plant, determination of optimum cycle for Sabalan power plant exhaust.* Geothermics **70**(2017), 181–191.

[35] Zanellato L., Astolfi M., SerafinoA., Rizzi D., Macchi E.: *Field performance ealuation of ORC geothermal power plants using radial outflow turbines.* Energy Procedia **129**(2017), 607–614.

[36] Gingerich D.B., Mauter M.S.: *Quantity, quality, and availability of waste heat from United States thermal power generation.* Environ. Sci. Technol. **49**(2015), 14, 8297–8306.

[37] Chen C.L., Li P.Y., Le S.N.T.: *Organic Rankine cycle for waste heat recovery in a refinery.* Ind. Eng. Chem. Res. **55**(2016), 3262–3275.

[38] Sun W., Yue X.: *Exergy efficiency analysis of ORC (organic Rankine cycle) and ORC based combined cycles driven by low-temperature waste heat.* Energ. Convers. Manage. **135**(2017), 63–73.

[39] Grover VI. Kyoto Protocol. Encyclopedia of Global Warming and Climate Change. SAGE Publications Inc. Thousand Oaks, CA.

[40] Grover VI. Montreal Protocol. Encyclopedia of Global Warming and Climate Change. SAGE Publications Inc. Thousand Oaks, CA.

[41] Le V.L., Feidt M., Kheiria A., Pelloux-Prayerb S.: *Performance optimization of low-temperature power generation by supercritical ORCs (organic Rankine cycles) using low GWP (global warming potential) working fluids.* Energy **67**(2014), 513–26.

[42] Aljundi I.H.: *Effect of dry hydrocarbons and critical point temperature on the efficiencies of organic Rankine cycle.* Renew. Energ. **36**(2011), 4, 1196–1202.

[43] Sprouse Iii C., Depcik C.: *Review of organic Rankine cycles for internal combustion engine exhaust waste heat recovery.* Appl. Therm. Eng. **51**(2013), 1-2, 711-722.

[44] Bracco R., Clemente S., Micheli D., Reini M.: *Experimental tests and modelization of a domestic-scale ORC (organic Rankine cycle).* Energy **58**(2013), 107–116.

[45] Wang X.D., Zhao L., Wang J.L., Zhang W.Z., Zhao X.Z., Wu W.: *Performance evaluation of a low-temperature solar Rankine cycle system utilizing R245fa.* Sol. Energy **84**(2010), 3, 353–364.

[46] Nguyen V.M., Doherty P.S., Riffat S.B.: *Development of a prototype low temperature Rankine cycle electricity generation system.* Appl. Therm. Eng. **21**(2001), 2, 169–181.

[47] Chintala V., Kumar S., Pandey J.K.: *A technical review on waste heat recovery from compression ignition engines using organic Rankine cycle.* Renew. Sust. Energ. Rev. **81**(2018), 1, 493–509.

[48] Astolfi M., Romano M.C., Bombarda P., Macchi E.: *Binary ORC (organic Rankine cycles) power plants for the exploitation of medium-low temperature geothermal sources – Part B: Techno-economic optimization.* Energy **66**(2014), 435–446.

[49] Fiaschi D., Manfrida G., Maraschiello F.: *Design and performance prediction of radial ORC turbo expanders.* Appl. Energ. **138**(2015), 517–532.

[50] Fiaschi D., Manfrida G., Maraschiello F.: *Thermo-fluid dynamics preliminary design of turbo-expanders for ORC cycles.* Appl. Energ. **97**(2012), 601–608.

[51] Pei G., Li J., Li Y., Wang D., Ji J.: *Construction and dynamic test of a small-scale organic Rankine cycle.* Energy **36**(2011),5, 3215–3223.

[52] Kang S.H.: *Design and preliminary tests of ORC (organic Rankine cycle) with two-stage radial turbine.* Energy **96**(2016), 142–154.

[53] Qiu G., Liu H., Riffat S.: *Expanders for micro-CHP systems with organic Rankine cycle.* Appl. Therm. Eng. **31**(2011), 16, 3301-3307.

[54] Zhang Y-Q., Wu Y-T., Xia G-D., Ma C-F., Ji W-N., Liu S-W., *et al.*: *Development and experimental study on organic Rankine cycle system with single-screw expander for waste heat recovery from exhaust of diesel engine.* Energy **77**(2014), 499–508.

[55] Imran M, Usman M, Park B-S, Lee D-H.: *Volumetric expanders for low grade heat and waste heat recovery applications.* Renew. Sust. Energ. Rev. **57**(2016), 1090–1109.

[56] Kaczmarczyk T.Z., Żywica G., Ihnatowicz E.: *The impact of changes in the geometry of a radial micro turbine stage on the efficiency of the micro CHP plant based on ORC.* Energy DOI: 10.1016/j.energy.2017.05.166.

[57] Walraven D., Laenen B., D'Haeseleer W.: *Comparison of shell-and-tube with plate heat exchangers for the use in low-temperature organic Rankine cycles.* Energ. Convers. Manage. **87**(2014), 227–237.

[58] Bao H., Wang Y., Charalambous C., Lu Z., Wang L., Wang R., Roskilly A.P.: *Chemisorption cooling and electric power cogeneration system drivenby low grade heat.* Energy **72**(2014), 590–598.

[59] Jiang L., Wang L.W., Zhang X.F., Liu C.Z.: *Performance prediction on a resorption cogeneration cycle for power and refrigeration with energy storage.* Renew. Energ. **83**(2015), 1250–1259.

[60] Lu Y., Lu Y., Wang Y., Bao H., Yuan Y., Wang L., Roskilly A.P.: *Analysis of an optimal resorption cogeneration using mass and heat recovery processes.* Appl. Energ. **160**(2015), 892–901.

[61] Jiang L., Wang L.W., Liu C.Z.,Wang R.Z.: *Experimental study on a resorption system for power and refrigeration cogeneration.* Energy **97**(2016), 182–190.

[62] Wang L., Roskilly A.P., Wang R.: *Solar powered cascading cogeneration cycle with ORC and adsorption technology for electricity and refrigeration.* Heat Transfer Eng. **35**(2014), 11-12, 1028–1034.

[63] Lu Y., Wang Y., Dong C., Wang L.W.: *Design and assessment on a novel integrated system for power and refrigeration using waste heat from diesel engine.* Appl. Therm. Eng. **91**(2015), 591–599.

[64] Sun W., Yue X.: *Exergy efficiency analysis of ORC (organic Rankine cycle) and ORC based combined cycles driven by low-temperature waste heat.* Energ. Convers. Manage. **135**(2017), 63–73.

[65] Tchanche B.F., Pétrissans M., Papadakis G.: *Heat resources and organic Rankine cycle machines.* Renew. Sust. Energ. Rev. **39**(2014), 1185–1199.

[66] Al-Mousawi F.N., Al-Dadah R., Mahmoud S.: *Novel system for cooling and electricity: Four different integrated adsorption-ORC configurations with two expanders.* Energ. Convers. Manage. **152**(2017), 72–87.

[67] Aphornratana S., Sriveerakul T.: *Analysis of a combined Rankine-vapor-compression refrigeration cycle.* Energ. Convers. Manage. **51**(2010), 2557–2564.

[68] Wang H., Peterson R., Harada K., Miller E., Ingram-Goble R., Fisher L., Yih J., Ward C.: *Performance of a combined organic Rankine cycle and vapor compression cycle for heat activated cooling.* Energy **36**(2011), 447–458.

[69] Toujeni N.,Bouaziz N.,Kairaouani L.: *Energetic investigation of a new combined ORC-VCC system for cogeneration.* Energy Procedia **139**(2017), 670–675.

[70] Saleh B., Koglbauer G., Wendland M., Fischer J.: *Working fluids for low-temperature organic Rankine cycles.* Energy **32**(2007), 1210–1221.

[71] Nasir M.T., Kim K.C.: *Working fluids selection and parametric optimization of an organic Rankine cycle coupled vapor compression cycle (ORC-VCC) for air conditioning using low grade heat.* Energ. Buildings **129**(2016), 378–395, DOI.org/10.1016/j.enbuild.2016.07.068

[72] EES, Enineering Equation Solver: ww.fchart.com/ees/

[73] Statgraphics: ww.statgraphics.com